Molecular Biology of the Cell
Vol. 10, 1821–1836, June 1999

# Amino Acid Sequence Requirements of the Transmembrane and Cytoplasmic Domains of Influenza Virus Hemagglutinin for Viable Membrane Fusion

**Grigory B. Melikyan,* Sasa Lin,† Michael G. Roth,† and Fredric S. Cohen*‡**

*Department of Molecular Biophysics and Physiology, Rush Medical College, Chicago, Illinois 60612; and †Department of Biochemistry, University of Texas Southwestern Medical Center at Dallas, Dallas, Texas 75235-9038

Submitted January 29, 1999; Accepted March 19, 1999
Monitoring Editor: Guido Guidotti

The amino acid sequence requirements of the transmembrane (TM) domain and cytoplasmic tail (CT) of the hemagglutinin (HA) of influenza virus in membrane fusion have been investigated. Fusion properties of wild-type HA were compared with those of chimeras consisting of the ectodomain of HA and the TM domain and/or CT of polyimmunoglobulin receptor, a nonviral integral membrane protein. The presence of a CT was not required for fusion. But when a TM domain and CT were present, fusion activity was greater when they were derived from the same protein than derived from different proteins. In fact, the chimera with a TM domain of HA and truncated CT of polyimmunoglobulin receptor did not support full fusion, indicating that the two regions are not functionally independent. Despite the fact that there is wide latitude in the sequence of the TM domain that supports fusion, a point mutation of a semiconserved residue within the TM domain of HA inhibited fusion. The ability of a foreign TM domain to support fusion contradicts the hypothesis that a pore is composed solely of fusion proteins and supports the theory that the TM domain creates fusion pores after a stage of hemifusion has been achieved.

## INTRODUCTION

Membrane fusion is common to many cellular processes, such as exocytosis and intracellular trafficking. But only in the case of viruses have the proteins responsible for fusion been unambiguously identified. A number of common features have been found among viral fusion proteins. All are oligomerized. The monomer of each oligomer always contains a critical stretch of nonpolar amino acids, known as the fusion peptide (Hernandez *et al.*, 1996; Durell *et al.*, 1997). As crystallographically determined, fusion proteins from several different virus families have the same backbone structure of extended coiled-coil $\alpha$-helices (Bullough *et al.*, 1994; Chan *et al.*, 1997). Because viral fusion proteins of unrelated viruses have common structural patterns, it is logical to assume that their mechanisms of fusion are similar as well. Furthermore, a complex of SNARES, proteins thought to be responsible for the constitutive fusion of intracellular trafficking and the regulated fusion that occurs in exocytosis (Südhof, 1995), has been crystallographically determined (Poirier *et al.*, 1998; Sutton *et al.*, 1998). It too displays a long coiled-coil region. Therefore it may well be that the mechanisms of viral fusion pertain more generally to cellular fusion. Influenza virus has long been the prototypic virus for study of fusion mechanisms. It

‡ Corresponding author. E-mail address: fcohen@rush.edu.

Abbreviations used: CF, carboxyfluorescein; CPZ, chlorpromazine; CT, cytoplasmic tail; DMEM, Dulbecco's modified Eagle's medium; GPI, glycosylphosphatidylinositol; HA, hemagglutinin; PBS-A-S, PBS supplemented with 0.1% sodium azide and 5% calf serum; p.i., postinfection; pIgR, polyimmunoglobulin receptor; R18, octadecylrhodamine B; RBC, red blood cell; RD, tetramethylrhodamine-tagged dextran; TM, transmembrane; VSV, vesicular stomatitis virus; WT, wild-type.

binds to cells via its hemagglutinin (HA). After binding, the virus is internalized within an endosome, where low pH causes conformational changes in HA that lead to fusion of the viral envelope with the endosomal membrane (Hernandez *et al.*, 1996). HA is a homotrimer with each monomer consisting of ~550 amino acid residues. Each monomer of HA has been conceptually divided into three domains: the ectodomain of ~515 residues constitutes the extraviral part of the molecule; a single stretch of 27 residues defines the transmembrane (TM) domain; and ~10 residues constitute the cytoplasmic tail (CT).

Cells that express on their surfaces a glycosylphosphatidylinositol (GPI)-anchored ectodomain of HA (i.e., ectodomain devoid of its TM domain and CT) hemifuse to target membranes at low pH (Kemble *et al.*, 1994; Melikyan *et al.*, 1995; Blumenthal *et al.*, 1996; Nüssler *et al.*, 1997; Chernomordik *et al.*, 1998). In hemifusion, the contacting monolayers of the two membranes merge, whereas previously noncontacting monolayers remain distinct but abut each other to form a single bilayer that continues to keep the aqueous compartments separate. At this stage all that remains for fusion to be completed is for a pore to form in the hemifusion diaphragm (i.e., in the single bilayer). Because GPI-HA yields hemifusion but not full fusion, the TM domain, absent in the construct, must be necessary for HA's fusion pore formation. If fusion proceeds from hemifusion, precise sequences within the TM domain and/or the CT might not be necessary for fusion pore formation. The CT of HA is not required for fusion (Jin *et al.*, 1994; Melikyan *et al.*, 1997b), and some foreign CTs have been substituted without significantly impairing fusion (Schroth-Diez *et al.*, 1998). Nevertheless, altering the CT can affect fusion to the point of abolishing it (Ohuchi *et al.*, 1998). Unlike the CT, the presence of the TM domain is essential, but the TM domain of other viral fusion proteins can substitute for that of HA (Schroth-Diez *et al.*, 1998).

For G protein (the fusion protein of vesicular stomatitis virus [VSV]) or gp160 (the fusion protein of human immunodeficiency virus), substituting the TM domains of nonviral integral membrane proteins, supported fusion (Wilk *et al.*, 1996; Odell *et al.*, 1997). This suggests that the mere presence of a TM domain is all that is necessary for fusion. However, running counter to this conclusion is the observation that point mutations within the TM domain of G protein inhibit fusion, indicating that specific residues within this domain do play a role in whether fusion proceeds (Cleverly and Lenard, 1998). It was not known whether the TM domain functions independently of the CT or how mutations within a TM domain could affect fusion.

We tested whether a precise amino acid sequence of the TM domain of HA is necessary for fusion by constructing chimeras that included the intact ectodomain of HA coupled with the TM domain of either HA or a protein unrelated to fusion, polyimmunoglobulin receptor (pIgR). The CT consisted of either HA or pIgR or was deleted. (The CT of pIgR was truncated to 11 amino acid residues to match the length of the HA tail.) We found that the foreign TM domain supported fusion, but this ability depended on which CT it was linked to. This is consistent with the hypothesis that hemifusion is a bona fide intermediate of full fusion. It also indicates that the TM domain and CT are not independent functional entities. Because it had been shown that there are critical residues within the TM domain of the G protein of VSV (Cleverly and Lenard, 1998), we made point mutations within the TM domain of HA to see whether this were true for HA as well. We found that a particular point mutation, G520L, did abolish fusion, arresting the process before lipid mixing. This suggests that a structural motif within the TM domain of HA is critical for membranes to reconfigure into a fusion pore.

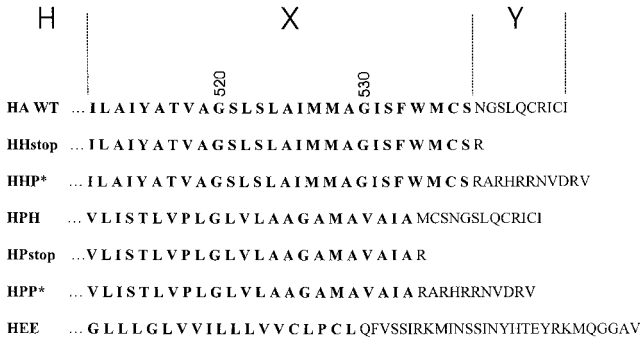


**Figure 1.** Amino acid sequences of the TM domains (bold) and CTs of Japan/305/57 HA WT and HA chimeras constructed for functional studies. The HA constructs are designated H-X-Y, where H is the ectodomain of HA, X is the origin of the TM domain (shown in bold letters), and Y the source of the CT. H denotes HA, P pIgR, and E the env protein of Rous sarcoma virus. A CT of P* symbolizes that the normal CT of pIgR was truncated to 11 amino acid residues to match the length of the CT of HA.

## MATERIALS AND METHODS

### *Construction and Expression of Influenza HA Chimeras*

The sequences of TM and cytoplasmic domains of the wild-type A/Japan/305/57 HA and six mutant or chimeric HA proteins are shown in Figure 1. Chimeras are designated H-X-Y, where H is always the HA ectodomain, X is the TM domain, and Y is the CT. P denotes the rabbit pIgR (Mostov *et al.*, 1984), and E is the env protein from Rous sarcoma virus. For all constructs, other than HEE, the CT consisted of either HA or pIgR or was deleted. P* indicates that the CT of pIgR was truncated from its natural 103 amino acid residues to 11 residues to match the length of the HA tail. To create the truncated cytoplasmic domain P*, a stop codon was inserted after the first 11 codons of the CT. This created a highly charged CT that

lacks the internalization signal found in the intact pIgR. HHH is referred to simply as wild-type (WT) HA. The construction and characterization of HEE (Lazarovits *et al.*, 1990) and HHstop (HA tail−) (Naim and Roth, 1993) have been described previously. HPP* and HHP* were constructed by megaprimer PCR mutagenesis (Sarkar and Sommer, 1990) using an oligonucleotide that inserted a stop codon followed by a restriction endonuclease recognition sequence for *Bam*HI immediately after the codon for valine 663, the 11th amino acid of the pIgR CT. The template for HPP* was a cDNA for the chimeric HA, HPP, and for HHP* the template was the chimera HHP (Lazarovits *et al.*, 1990). *Xba*I–*Bam*HI fragments containing the chimeric sequences were used to replace the wild-type *Xba*I–*Bam*HI fragment in the SV40 expression vector pkSVEHAxba−, in which the *Xba*I site at HA nucleotide 145 has been destroyed by a silent mutation. To construct HPH, an oligonucleotide containing 17 nucleotides encoding the last amino acids of the pIgR TM domain and the first 19 nucleotides encoding the beginning of the HA CT was used to prime synthesis on a wild-type HA template, producing a fragment in which pIgR sequence was joined to sequences encoding the CT of HA. This fragment was then used to prime synthesis on a template of HPP. After digestion with restriction nucleases, a *Bam*HI–*Xba*I fragment encoding portions of the HA external domain, the pIgR TM, and the HA CT was subcloned into SVEHA as described above. To make HPstop, an oligonucleotide was synthesized that contained the last 18 nucleotides of the antisense strand of the pIgR TM coding region preceded by a stop codon and a *Bam*HI endonuclease recognition site at the 5′ end. This was used with a template of pkSVEHPP to prime synthesis of a fragment spanning the HPP region between the remaining *Xba*I site in HA and the codon for the first arginine of the pIgR CT. This was subcloned into pkSVEHAxba− as described above. For all recombinant viruses, the sequence of the DNA between the *Xba*I and *Bam*HI sites was determined after the subcloning step. Recombinant virus stocks for expressing each of the proteins were prepared by transfecting DNAs for the recombinant viruses and for the helper virus DL1055 together into CV-1 cells and then culturing viruses in cell lysates one or more times (Naim and Roth, 1994). Virus stocks between passage two and passage four were used for experiments.

## Analysis of HA Expression and Folding

The ability of proteins HEE and HHstop (HAtail−) to fold and oligomerize correctly has been established previously (Lazarovits *et al.*, 1990; Naim and Roth, 1993). The folding of chimeric HAs was monitored by pulse–chase experiments as described (Naim and Roth, 1994). CV-1 cells that had been infected with SV40 vectors for 30 h were labeled with 200 $\mu$Ci/ml Trans$^{35}$Slabel (ICN, Irvine, CA) for 15 or 30 min at 37°C in Dulbecco's modified Eagle's medium (DMEM) lacking cysteine and methionine. Cells that had been labeled for the shorter period were chased for 0, 40, or 80 min at 37°C in DMEM containing 10 $\mu$g/ml trypsin. Cells labeled for 30 min were chased for 60 min at 37°C in DMEM and then were treated at 4°C for 45 min with DMEM containing 100 $\mu$g/ml trypsin. For either type of chase, trypsin was removed, and the cells were rinsed with DMEM containing 5% FBS and then were incubated in PBS containing 100 $\mu$g/ml soybean trypsin inhibitor. The cells were then lysed, and the HAs were immunoprecipitated (Naim and Roth, 1994). Immunoprecipitated HA0, HA1, and HA2 were separated by PAGE and both visualized and quantified by PhosphorImager (Molecular Dynamics, Sunnyvale, CA).

The relative expression of WT and chimeric HAs on the surface of CV-1 cells was assessed by flow cytometry. At 42 h postinfection (p.i.) cells were detached from the dish and resuspended in PBS supplemented with 0.1% sodium azide and 5% calf serum (PBS-A-S). Cells were incubated with the mAb FC-125 against Japan/305/57 HA diluted 1:20 in PBS-A-S for 45 min on ice (FC-125 mAb was a generous gift of Dr. T. Braciale, University of Virginia, Charlottesville, VA). Cells were then washed with PBS-A-S, exposed to FITC-conjugated goat anti-mouse antibody (Southern Biotechnology Associates, Birmingham, AL) diluted 1:100 for 45 min on ice, fixed with 2% methanol-free paraformaldehyde (Electron Microscopy Sciences, Ft. Washington, PA), and analyzed with a flow cytometer (ORTHO Cytoron Absolute; Ortho Diagnostic Systems, Raritan, NJ). The fluorescence background attributable to nonspecific binding was determined by incubating infected cells with only FITC-conjugated secondary antibodies.

## Cholesterol Depletion

To determine whether treating cells with $\beta$-cyclodextrin to deplete them of cholesterol did change the affinity of HA for the detergent-insoluble membrane fraction, 39 h after infection with recombinant SV40 vectors expressing either wild-type or mutant HAs, CV-1 cells were labeled with 200 $\mu$Ci/ml Trans$^{35}$Slabel for 15 min and then chased in DMEM for 1 h (for functional experiments the cells were treated at 42 h p.i.). Half the samples were treated for 30 min at 37°C with DMEM containing 50 mM HEPES, pH 7.0, and the other half were treated with the same medium containing 10 mM methyl-$\beta$-cyclodextrin (Sigma, St. Louis, MO). The cells were washed twice with PBS containing 1 mM $Mg^{2+}$ and 0.5 mM $Ca^{2+}$ and incubated at 22°C for 10 min in the same solution containing 10 $\mu$g/ml trypsin. Soybean trypsin inhibitor was added to a final concentration of 10 $\mu$g/ml, and loose cells were centrifuged from the medium and added back to the cells remaining in culture dishes. Cells were lysed on ice in cold lysis buffer containing 50 mM Tris, pH 8.0, 0.1 U of aprotinin, 10 $\mu$g/ml soybean trypsin inhibitor, and 1% Triton X-100. The lysate was scraped into cold microfuge tubes and centrifuged at 4°C for 15 min at 14,000 $\times$ *g*. Each sample was separated into the Triton X-100–soluble supernatant and the insoluble pellet. Lysis buffer containing 0.1% SDS was added to the pellet for 1 h at 22°C with occasional vortexing. The remaining insoluble material was removed by centrifugation, and the SDS supernatant was collected. Both Triton X-100–soluble and –insoluble fractions were immunoprecipitated with rabbit anti-HA antibody and analyzed by PAGE and PhosphorImager as described above.

## Labeling Red Blood Cells

Freshly collected human red blood cells (RBCs) were colabeled with lipophilic and aqueous dyes as described (Melikyan *et al.*, 1995). Briefly, octadecylrhodamine B (R18) and 1,1′-dioctadecyl-3,3,3′3′-tetramethyl indocarbocyanine iodide were used as markers for HA-induced lipid mixing between RBCs and CV-1 cells expressing WT and chimeric HAs. Red cells labeled with a membrane dye were loaded with the aqueous dye carboxyfluorescein (CF) by mild hypotonic lysis (Ellens *et al.*, 1989). In separate experiments, RBCs were loaded only with aqueous dyes of different molecular weights: CF and tetramethylrhodamine-tagged dextran (RD; $M_r$ 40,000). All fluorescent dyes were purchased from Molecular Probes (Eugene, OR).

## Cell–Erythrocyte Dye Spread Experiments

A freshly confluent monolayer of CV-1 cells was infected with recombinant SV40-HA virus stock (0.2–0.3 ml of SV40-HA stock/6-cm culture dish) as described (Naim and Roth, 1994). At 39 h p.i., infected cells were taken off dishes by a brief (<1 min) incubation with a 0.5 mg/ml solution of trypsin in PBS containing 0.5 mM EDTA. Cells were seeded on 35-mm culture dishes, placed in a 5% $C0_2$ incubator, and used for experiments between 42 and 44 h p.i. Just before an experiment, cells were treated with 0.2 mg/ml neuraminidase (type V, from *Clostridium perfringens*) and 10 $\mu$g/ml *N*-tosyl-L-phenylalanine chloromethyl ketone–treated trypsin (both enzymes purchased from Sigma) in PBS for 10 min at room temperature to ensure complete cleavage of HA0 into HA1–HA2 subunits. The reaction was stopped with an excess of serum-supplemented medium. Cells were then washed three times with PBS and incubated 10 min at room temperature with 1 ml of a 0.0025%

suspension of labeled RBCs with occasional rocking. Unbound red cells were removed by washing three times with PBS. When binding was quantified, the number of RBCs attached to every CV-1 cell in several randomly selected fields was counted. Fusion was triggered by applying the pH 4.8 solution used for patch-clamp experiments (see below) for 2 min at the indicated temperature. The pH 4.8 solution was replaced with isotonic PBS supplemented with 20 mM D-raffinose to prevent colloidal-osmotic swelling of the RBCs that could be induced by HA-mediated leakage. Cells were kept at neutral pH for 5–10 min before examining the extent of fusion. In experiments in which low fusion activity was observed, cells were treated with 0.5 mM of chlorpromazine (CPZ; Sigma) in PBS containing 20 mM raffinose.

Detection of spread of cytoplasmic and/or membrane dye from RBCs to HA-expressing cells (referred to as HA cells) was performed as described previously (Melikyan *et al.*, 1995, 1997b). Briefly, different parts of a culture dish were selected at random, and the number of HA-expressing cells stained with membrane and/or aqueous dye was normalized by the total number of cells in the microscopic fields with at least one attached RBC. On average, ~100 cells were screened per culture dish. The spread of fluorescent markers was monitored under a microscope (Axiovert 100; Carl Zeiss, Thornwood NY) equipped with an intensified (KS1380; Video Scope, Washington, DC) charge-coupled device video camera (model 72; Dage, Michigan City, IN). The output of the video camera was recorded on S-VHS format videotape for later analysis. Images were digitized off-line by a video frame grabber (Meteor; Matrox Electronic Systems, Dorval, Quebec, Canada) and a PC-based computer.

### *Electrical Measurements*

For electrophysiological experiments HA-expressing cells were removed from the culture dishes 41 h after infection, allowed to attach to No. 1.5 cover glasses for 1 h in a 5% $CO_2$ incubator, treated with a neuraminidase-trypsin mixture, and decorated with RBCs as described above. Cells were stored at 4°C and transferred into an experimental chamber containing (in mM) 150 *N*-methylglucamine aspartate, 5 $MgCl_2$, and 2 Cs-HEPES, pH 7.2. The same solution but buffered with 20 mM Cs-succinate, pH 4.8, was used to trigger fusion. Patch pipettes were filled with (in mM) 155 Cs glutamate, 5 $MgCl_2$, 5 bis(2-aminophenoxy)ethane-*N*,*N*,*N*′,*N*′-tetraacetic acid, and 10 Cs-HEPES buffer, pH 7.4 (Spruce *et al.*, 1989; Spruce *et al.*, 1991). Fusion was triggered by ejecting the pH 4.8 solution from another micropipette placed ~70 $\mu$m from the cell. Unless otherwise specified, patch-clamp experiments were conducted at room temperature. Formation and enlargement of the fusion pore between RBC and HA-expressing cell was monitored in the whole-cell patch-clamp configuration by time-resolved admittance measurements essentially as described (Spruce *et al.*, 1991; Tse *et al.*, 1993). Briefly, capacitance transients were canceled by adjusting the whole-cell capacitance and series resistance compensation potentiometers (Axopatch 200B; Axon Instruments, Foster City, CA). The command voltage was generated, and resulting currents were analyzed by a software-based lock-in program (Ratinov *et al.*, 1998). A sine wave (200 Hz, 50 mV peak-to-peak) superimposed on −40 mV potential was applied to the pipette. The output of the patch-clamp amplifier was filtered by a four-pole Bessel filter at 5 kHz and digitized at 40 kHz using a 16-bit analog-to-digital board (PC-44; Innovative Integration, Westlake Village, CA). The software-based lock-in amplifier calculated the DC conductance ($Y_{DC}$), as well as the in-phase ($Y_0$) and out-of-phase ($Y_{90}$) components of admittance for each period of sine wave, saving directly to a hard disk. The specific phase angle for lock-in measurements (Joshi and Fernandez, 1988; Gillis, 1995) was found by "capacitance dithering" (Neher and Marty, 1982). Fusion pore conductances were calculated off-line as $G_P = (Y_0^2 + Y_{90}^2)/Y_0$ (Lindau, 1991; Ratinov *et al.*, 1998). The evolution of the average pore conductance was characterized by aligning individual pore conductance records at the moment of pore opening and calculating a mean pore conductance every 5 or 20 ms. For some pores, conductances increased beyond measurable values, usually ~20 nS, sooner than the time interval selected to build the average pore profile (e.g., 20 s). In these cases the last value of pore conductance that could be reliably calculated was used for the rest of the time interval to calculate the average conductance. Because the conductance of enlarged pores almost always tends to further increase, the mean distribution of pore conductances is increasingly biased toward the more slowly enlarging pores as time proceeds.

## RESULTS

### *Chimeras with Foreign TM Domains Are Properly Folded, Transported, and Expressed*

HA is a trimeric protein that rapidly folds and oligomerizes in the endoplasmic reticulum to form a protease-resistant protein that is cleaved by trypsin at a single site on each monomer. Unfolded or partially folded HAs reveal additional trypsin cleavage sites and produce a more complicated series of fragments when treated with the protease. Thus, the ability of a chimeric HA to be cleaved by trypsin into only HA1 and HA2 is a sensitive measure of the correct folding of the HA external domain (Copeland *et al.*, 1986; Gething *et al.*, 1986; Lazarovits *et al.*, 1990). To determine whether chimeric HAs folded properly, the proteins were expressed in CV-1 cells infected with SV40 expression vectors, and the proteins were analyzed by pulse-chase protocols. Two variations of these experiments are shown in Figure 2. Either cells were pulse labeled with $^{35}$S-amino acids and chased at 37°C for various periods in DMEM containing trypsin (Figure 2A), or cells were labeled and chased at 37°C in the absence of trypsin and were then treated at 4°C with trypsin in PBS (Figure 2B). HA proteins were immunoprecipitated from the cell lysates and analyzed by PAGE. At the end of the labeling period, partially folded HA monomeric chains were sensitive to proteolytic degradation, producing a series of discrete bands migrating faster than HA0 on the gel (Figure 2A, lanes 1 and 4). After periods long enough for proteins to reach the cell surface (40–80 min), HA WT or HPP* proteins were cleaved by the trypsin in the culture medium into HA1 and HA2 subunits. As the chase progressed, less HA0 remained within the cell, and more HA1 and HA2 was produced (Figure 2A, lanes 2, 3, 5, and 6). Both HPP* and HA WT moved to the cell surface at a similar rate and exhibited similar resistance to degradation by trypsin. A similar result was observed for HHP* (Figure 2B, lane 2), HPH, and HPstop (our unpublished results). Although the proteins lacking the CT traveled more slowly to the cell surface, once they arrived there they were as resistant to degradation by trypsin as was HA WT. Similar results have been reported for HEE and HHstop (Lazarovits *et al.*, 1990; Naim and Roth, 1993).

The expression levels of WT and chimeric HAs on surfaces of CV-1 cells infected by SV40-HA were measured by flow cytometry 42 h p.i. The fraction of cells

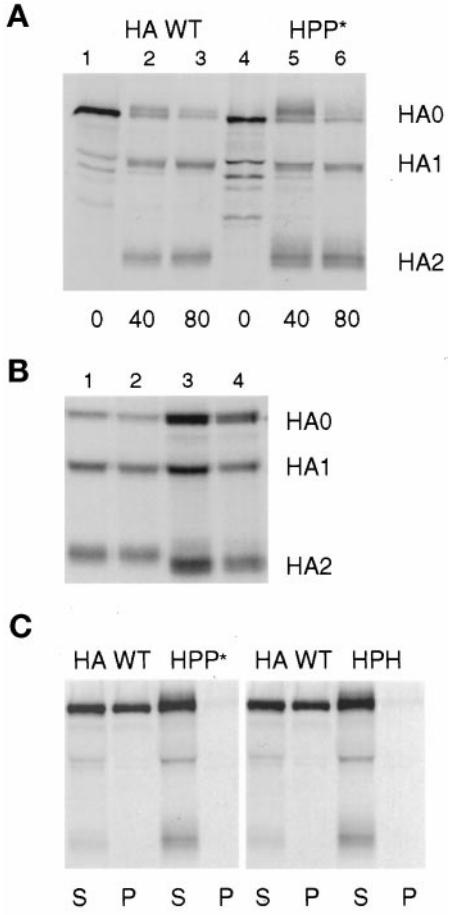


**Figure 2.** Characterization of the folding and detergent solubility of chimeric HA proteins. (A) CV-1 cells infected with SV40 vectors expressing HA WT or HPP* were pulse labeled for 15 min and chased for the intervals shown in serum-free DMEM containing 10 $\mu$g/ml trypsin. Samples were lysed with both Triton X-100 and SDS and immunoprecipitated. HA0, HA1, and HA2 bands were separated by PAGE under reducing conditions. (B) Cells were pulse labeled for 30 min and chased in DMEM for 60 min and then were treated with trypsin in PBS for 60 min at 4°C. Samples were lysed, precipitated, and analyzed as in A. Lane 1, HA WT; lane 2, HHP*; lane 3, HA G530W; lane 4, HA G520L. (C) Cells were labeled with radioactive amino acids for 15 min and chased for 60 min. The cells were then incubated 10 min at 22°C in PBS containing trypsin to cleave HA at the cell surface into HA1 and HA2 subunits. The cells were lysed with Triton X-100 at 4°C, and sample lysates were separated by centrifugation into supernatant (S) and pellet (P) fractions. The pellets were then solubilized by the addition of SDS, and both S and P fractions were immunoprecipitated with antibodies specific for HA. For A–C, digital images of PhosphorImager scans of the dried gels are shown.

expressing HA and the mean fluorescence intensities were comparable for WT HA and the chimeric constructs (Table 1). Mutations in HA or substitutions of the TM domain and CT by those of another protein can potentially affect the glycosylation of the ectodomain. This, in turn, could inhibit HA binding to sialic acid–bearing receptors on the erythrocyte surface

**Table 1.** Expression levels of WT HA and chimeras in CV-1 cells as determined by flow cytometry

| HA expressed | Expressing cells (%) | Mean fluorescence (a.u.) | Average number of RBC bound |
|---|---|---|---|
| WT (HHH) | 54 ± 6 | 27 ± 7 (100)[a] | 2.3 |
| HHstop | 61 ± 14 | 24 ± 9 (89) | 1.3 |
| HHP* | 59 ± 5 | 26 ± 1 (96) | 2.1 |
| HPP* | 63 ± 8 | 31 ± 9 (115) | 2.2 |
| HPstop | 60 ± 19 | 21 ± 6 (78) | 1.7 |
| HPH | 51 ± 4 | 20 ± 3 (74) | 1.8 |
| HEE | 59 ± 8 | 39 ± 11 (144) | 2.1 |
| G530W | 21 | 9.4 (35)[b] | ND |
| G520L | 51 ± 9 | 29 ± 13 (107) | 1.9 |

Data are shown as a mean of three to eight independent experiments ± SE. Cells were used for flow cytometry experiments at 42 h after infection with recombinant SV40HA virus as described in MATERIALS AND METHODS. a.u., arbitrary unit; ND, not determined.

[a] Normalized to mean fluorescence intensity of WT HA.

[b] For the G530W mutant we did not attempt to bring the expression closer to that of WT HA, because the fusion phenotype was not altered appreciably even at this lower expression level. Only two measurements of the expression level were carried out in this case.

(Kemble *et al.*, 1993). But the average number and the distribution (between 0 and 8 under our experimental conditions) of bound RBCs per HA-expressing cell were similar for all HA constructs (Table 1). This and the equivalent gel migration of the glycosylated HA1 subunit for WT HA and chimeras (Figure 2) indicate that all constructs were normally glycosylated. Thus the folding, the levels of expression, and the binding of RBCs were comparable for all forms of HA.

### *The TM Domain of an Integral Membrane Protein Unrelated to Fusion Still Supports Fusion*

RBC ghosts fluorescently colabeled with a membrane (R18) and an aqueous (CF) dye were bound to HA cells adhered to plastic culture dishes. After a 2-min low-pH pulse followed by reneutralization, fusion was monitored by the transfer of the lipidic (Figure 3, left panel) and aqueous dye (Figure 3, right panel) to adjacent HA cells. For all constructs tested, except HHP*, both lipid and aqueous dye transferred efficiently, as illustrated for WT HA, HEE, and HPP* (Figure 3, see MATERIALS AND METHODS for description of notation). In all cases, if the HA0 expressed on CV-1 cell surfaces were not previously cleaved by trypsin into its active HA1–HA2 form, neither membrane nor aqueous dye transferred (our unpublished results). Most importantly, we found that a foreign TM domain was functional not only in the presence of its own CT (HPP*) but also in the absence of a CT (HPstop) or in the presence of the CT of HA (HPH). Although the presence of a CT is not required

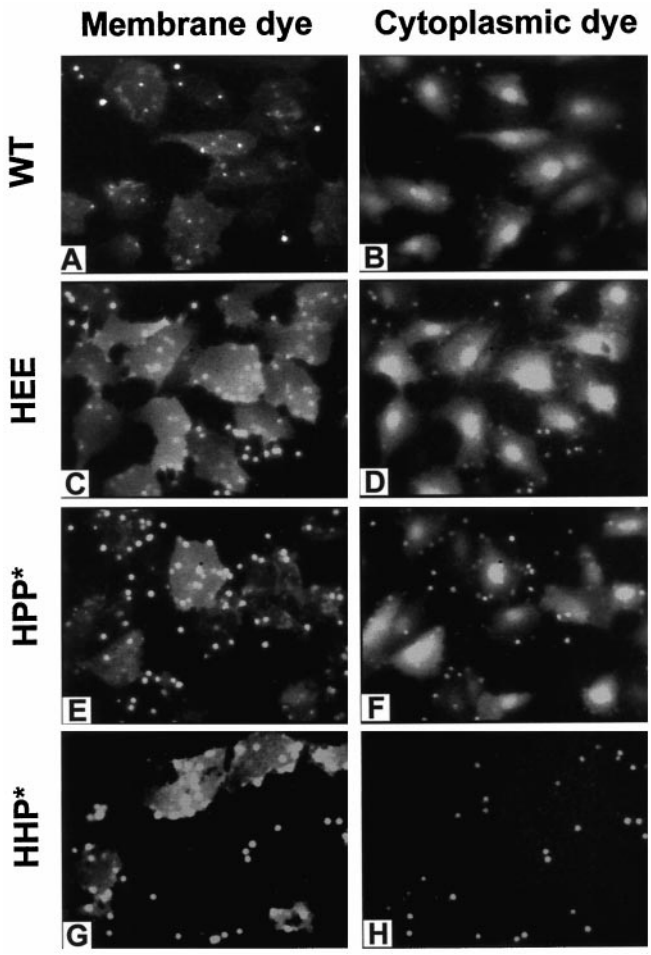


**Figure 3.** Membrane and aqueous dye mixing activity of WT HA and the HEE, HPP*, and HHP* chimeras. All constructs induced R18 to redistribute from RBCs to cells expressing the constructs (left panel). The cytoplasmic marker (CF) transferred efficiently for WT HA and HEE- and HPP*-expressing cells (right panel), demonstrating fusion. In contrast, HHP* only supported limited transfer of a membrane dye without transfer of aqueous dye, suggesting that it caused hemifusion. RBC ghosts colabeled with R18 and CF were bound to HA cells, and fusion was triggered by a 2-min application of pH 4.8 buffer at 37°C, followed by incubation for 5–8 min at neutral pH before microscopically examining cells.

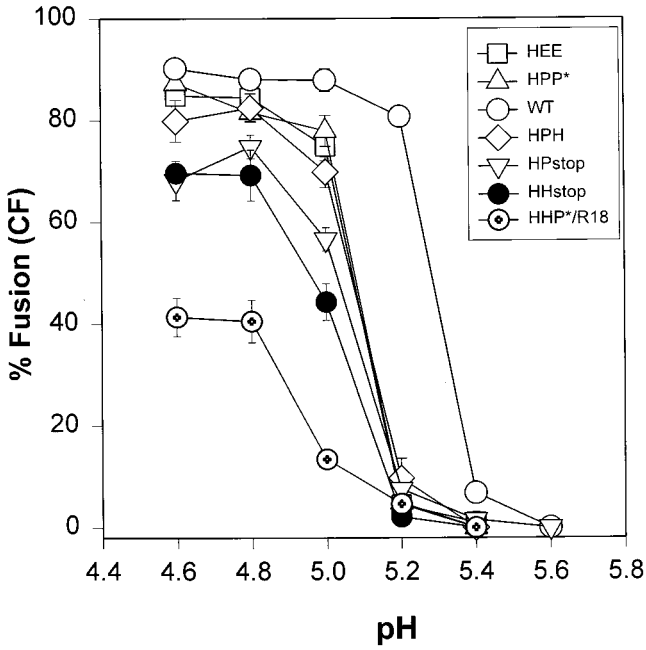


**Figure 4.** pH dependence of fusion induced by WT and chimeric HA. Fusion between HA-expressing CV-1 cells and RBC ghosts colabeled with CF and R18 was triggered by application of an acidic buffer of the indicated pH for 2 min at 37°C followed by incubation in PBS supplemented with 20 mM raffinose for 5 min at room temperature. For the HHP* construct, the incubation at neutral pH was extended to 15 min. Every point on the graph corresponds to a mean value obtained from four to eight independent experiments (bars indicate SE). The steep pH dependence of WT HA-induced fusion (open circles) was found for all HA chimeras, although the pH curve for the chimeras was shifted by ~0.2 units toward more acidic pH. Because of the virtual absence of CF transfer for the HHP* construct, its pH dependence is shown for R18 mixing (circles with cross).

for fusion, a foreign CT can inhibit fusion; for HHP* only lipid (but not aqueous) dye transferred and then only into some cells (Figure 3, G and H). This is the pattern of dye spread expected of hemifusion but not full fusion. Subsequent addition of CPZ, a membrane-permeable tertiary amine, at relatively high concentrations (0.5 mM) promoted transfer of aqueous dye (our unpublished results); this is characteristic of the behavior of hemifused cells (Melikyan *et al*., 1997a).

All HA chimeras (except for HHP*) exhibited a similar pH dependence for CF transfer, but their thresholds were consistently shifted by ~0.2 units toward more acidic pH values than WT HA (Figure 4). For all constructs, transfer of CF was maximal and comparable when fusion was induced at pH 4.8. The pH dependence for R18 or 1,1′-dioctadecyl-3,3,3′3′-tetramethyl indocarbocyanine iodide mixing for all the fully functional HA chimeras was virtually identical to CF transfer (our unpublished results). The pH dependence of the HHP* chimera in inducing hemifusion (Figure 4, circles with cross) was similar to the pH dependence of fusion for the other chimeras, but even at pH 4.6 a relatively small fraction of HHP* cells received lipid dye.

### *The TM Domain and CT Do Not Act Independently of Each Other*

The extent of fusion can be quantified by measuring the fraction of cells that acquire dye. This provides a means to compare efficacy of pore formation by the different constructs. Enlargement of fusion pores to diameters exceeding the size of a viral nucleocapsid is essential for viral infection. Thus it is of interest to also

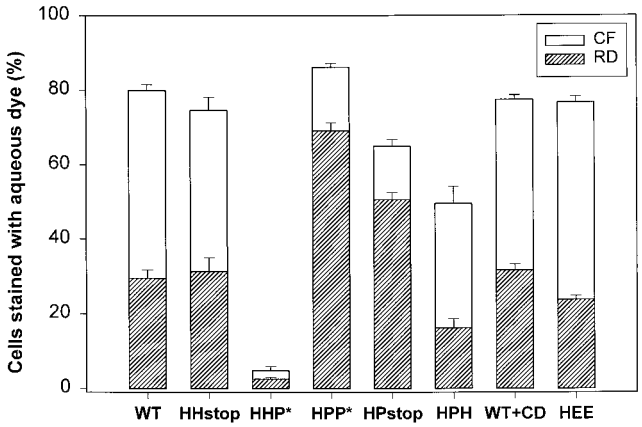


**Figure 5.** Fusion pore enlargement monitored by differential sieving of a large and small cytoplasmic dye. RBC ghosts coloaded with CF ($M_r$ 376) and RD ($M_r$ 40,000) were bound to HA-expressing CV-1 cells, and fusion was triggered by application of a pH 4.8 solution for 2 min at 23°C. Cells were then incubated in PBS with 20 mM raffinose for 5 min (15 min for HHP*) at neutral pH, and the fraction of cells stained by CF (open bars) and RD (striped bars) was determined by fluorescence microscopy. The HHP* chimera promoted virtually no content mixing. Depleting CV-1 cells of cholesterol by incubation with β-cyclodextrin did not affect either the formation or enlargement of WT HA pores. Error bars represent SE for 5–10 independent experiments.

examine pore enlargement. The "differential sieving" of a large and small aqueous dye (both smaller than the size of a nucleocapsid) by a pore provides a means to access whether some enlargement has occurred. RBC ghosts were coloaded with RD ($M_r$40,000) and CF ($M_r$ 376), and the ability of each to transfer to an HA cell was measured. For all HA constructs except HHP*, RD (Figure 5, striped bars) transferred (but to a smaller degree than CF, open bars), demonstrating that at least one fusion pore enlarged sufficiently to allow passage of the large fluorescent marker. The fraction of cells stained by CF that were also stained by RD varied among HA chimeras (Figure 5). The extent of small dye redistribution was the same for HPP* and WT HA cells. A greater fraction of HPP* cells acquired RD than did cells expressing other constructs, including WT HA. This indicates that fusion pores more readily enlarged with HPP*. Deleting the CT from WT HA did not affect pore formation or growth. Although deleting the CT from HPP* reduced both pore formation and growth, the effect was small and could have been due to the somewhat lower expression levels of HPstop (Table 1). Deleting the CT from HPH (yielding HPstop) clearly led to greater pore formation and growth. Most strikingly, HHP* did not support fusion. Thus, for each TM domain, pore formation and growth depended on which CT was present; similarly, the effect of the CT on fusion depended on which TM domain was present. In other words, fusion pore formation and enlargement vary with the combination of the TM domain and CT.

### *Partitioning into Rafts Does Not Affect Fusion Properties of HA*

Extracting HA trimers from cells by Triton X-100 or 3-[(3-cholamidopropyl)dimethylammonio]-1-propanesulfonic acid at 4°C yields 40 to 75% of the trimers in a detergent-insoluble membrane fraction (Figure 2C) rich in cholesterol and sphingomyelin (Schieffele *et al.*, 1997). The insolubility of membrane protein under these conditions is the biochemical assay used to identify the partitioning of protein into the microenvironment of rafts (Brown and London, 1997; Simons and Ikonen, 1997). (Rafts are small patches of the membrane rich in cholesterol and sphingomyelin [Friedrichson and Kurnachalia, 1998; Varma and Mayor, 1998].) HA trimers incorporated in cell membranes are thus thought to reside in rafts (Schieffele *et al.*, 1997). Although it has not been shown that HA definitely resides within rafts, it has been experimentally shown that the affinity of HA for detergent-insoluble fractions is determined by its TM sequence (Schieffele *et al.*, 1997). We tested whether functional differences between chimeras might be due to their lipid microenvironment. We depleted WT HA cells of cholesterol by incubating them with β-cyclodextrin (Lin *et al.*, 1998). The fraction of WT HA trimers found in the Triton X-100–insoluble pellet was reduced from 74 to 4% (our unpublished results), consistent with the elimination of rafts by cholesterol depletion (Schieffele *et al.*, 1997). But pore formation and enlargement induced by WT HA were not affected by the elimination of rafts (Figure 5, WT + CD). We found that neither HPP*, optimal for fusion, nor HPH, less effective for fusion than WT HA, partitioned into rafts: both were solubilized by detergent at 4°C (Figure 2C). Thus, whether the fusion protein constructs reside in rafts within cell membranes is immaterial to their fusion activity. However, we cannot rule out the possibility that the association of a small number of specific lipids with HA has some bearing on the fusion process.

### *The Fraction of Bound RBCs That Fuse Can Be Measured Electrically*

The finding that CF spread for all constructs except HHP* establishes that a foreign TM domain can substitute for that of HA in the fusion process. By the time the dye spread is observable, however, several processes have occurred: a pore has formed; it has enlarged enough to pass CF; and a quantity of dye molecules have moved. Therefore, dye spread measurements cannot reliably indicate the kinetics of pore formation. In addition, the differential sieving experiments show that CF and RD do not transfer to the same extent for all constructs (Figure 5). Because dye spread measurements cannot pinpoint where in the

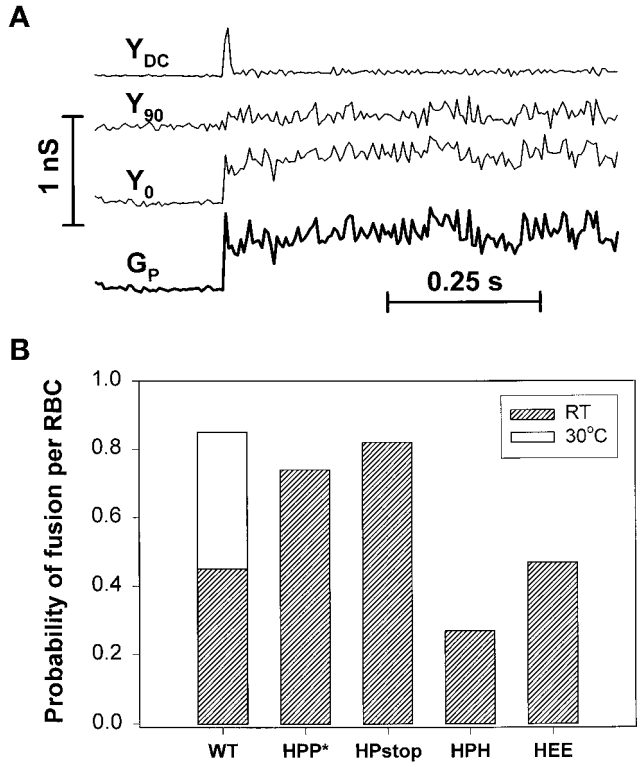


**Figure 6.** Characteristic electrical signals upon opening of a fusion pore between an RBC and a CV-1 cell and probability that a bound RBC did fuse. (A) The DC conductance ($Y_{DC}$) and in-phase ($Y_0$), and out-of-phase ($Y_{90}$) conductances were measured by the patch-clamp technique in a whole-cell mode, allowing the fusion pore conductance ($G_P$) to be calculated. The opening of a fusion pore was accompanied by a spike in DC conductance and changes in $Y_0$ and $Y_{90}$. (B) The number of current spikes in $Y_{DC}$ yields the number of RBCs that have fused to the cell. By counting the number of RBCs bound to the CV-1 cell, the probability of fusion per bound RBC was obtained.

process these differences lie, we augment the dye experiments with electrical measurements. These measurements record pores the instant they form and continue to profile their growth. Electrical measurements thus provide an accurate means to determine kinetics and extent of fusion.

HA cells were therefore patch clamped in the whole-cell mode, and fusion was detected by the addition of the capacitance of the RBC membrane to the HA cell through the fusion pore. The changes in electrical signals (the in-phase, $Y_0$, and out-of-phase, $Y_{90}$, admittance) upon pore formation (Figure 6A) allowed the fusion pore conductance, $G_P$, to be calculated (see MATERIALS AND METHODS). Each of the chimeras of this study proved suitable for this method, except for HHstop, which induced electrical leakage through the HA cell membrane, preventing reliable capacitance measurements. The ability of P as the TM domain to support fusion with different CTs (HPP*, HPH, and HPstop) was evaluated by electrical measurements.

In general, pore opening causes a sudden increase in DC that quickly decays (Figure 6A, transient in $Y_{DC}$; Spruce *et al.*, 1991), because the resting potential of an RBC and the holding potential of an HA cell are different. We found that when an HA cell had more than one bound RBC, the fusion of each of them resulted in a characteristic spike current. We realized that by counting the number of spikes, we could directly obtain the number of RBCs that fused to each HA cell.[1] This is the first procedure developed for measuring the efficiency of fusion when more than one RBC is bound. (Fluorescent dye spread measurements can show that at least one of the bound RBCs fused, but the precise number cannot be determined.) By this method we can now obtain the probability of fusion per RBC based on the ratio of the number of fused RBCs to those bound to a HA cell.

We found that the probability of fusion of an RBC was significantly higher for HPP* cells and HPstop cells than for WT, HEE, and HPH-expressing cells (Figure 6B). (This high probability for HPP* and HPstop suggests that they may induce several pores for each bound RBC.) The rate and extent of HA-mediated fusion is well known to increase dramatically with temperature (Stegmann *et al.*, 1990). At 30°C the efficiency of fusion for WT HA reached that of HPP* at room temperature. We have thus found that the effect of a TM domain on the efficiency of fusion depended on the amino acid sequence of the CT. Deleting the CT from WT (Melikyan *et al.*, 1997b) or HPP* (yielding HPstop) does not significantly alter fusion, whereas replacing the CT in HPP* by H (yielding HPH) lowers the efficiency of fusion by a factor of 3. Despite the fact that the same percentage of WT HA cells and HPP* cells acquired CF (Figure 5), the fraction of RBCs that fused was significantly higher for HPP*. Electrical measurements allow more definitive, less ambiguous, interpretations of data.

[1] The spike discharge current results from the charging of the RBC membrane capacitance, through the series resistance of a fusion pore, to the potential of the HA cell membrane. We always verified that these transients were due to fusion pore opening rather than due to spurious events, such as a transient leakage current through a cell membrane, by checking that the in-phase ($Y_0$) and out-of-phase ($Y_{90}$) signals changed (Figure 6A), as is characteristic of fusion pore formation. We tested the quantitative reliability of counting spikes to determine the number of RBCs that fused to an HA cell. As pores enlarged readily for HPP* cells, we could be reasonably certain that the full capacitance of each fused RBC was electrically revealed. The total increase in HA cell membrane capacitance should be approximately equal to the product of the number of current transients and the average RBC membrane capacitance of ~1 pF (Spruce *et al.*, 1989). This was the case.

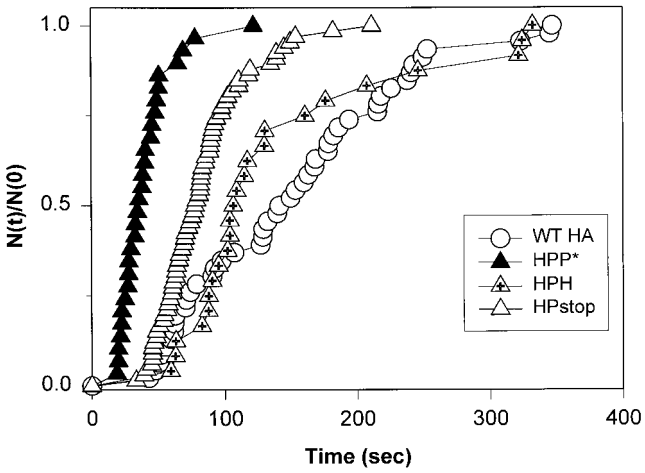


**Figure 7.** Kinetics of fusion between RBCs and HA cells. Fusion was triggered by exposing cells to a pH 4.8 solution for 2 min at room temperature. The waiting times until pore formation were determined electrically. These times were ranked for each construct and plotted as the cumulative distribution of the fraction of cells that have fused by time [i.e. N(t) of the total experimental pool of N(0)]. The kinetics of fusion was similar for WT HA (open circles) and HPH (triangles with cross), each slower than for HPP* (filled triangles) and HPstop (open triangles).

### *The Kinetics of Fusion Is Determined by the TM Domain and CT Together*

We determined the fusion kinetics for chimeras containing the TM domain of pIgR by electrically measuring the latencies between exposure of HA cells with bound RBCs to low pH and the opening of a fusion pore (Figure 7). The kinetics was much faster for HPP* (filled triangles) than for cells expressing WT HA on their surfaces (open circles). (HEE cells containing the membrane anchor of Rous sarcoma virus env protein induced fusion as fast as HPP* cells (our unpublished results).) Deletion of the CT tail of HPP* (HPstop; Figure 7, open triangles) resulted in somewhat slower kinetics (although this may well be due to the somewhat lower expression of HPstop); substituting the HPP* tail with that of HA (HPH; Figure 7, crossed triangles) significantly slowed fusion kinetics to the level of WT HA. However, the efficiency of pore formation was higher for WT HA than for HPH (Figure 6B); it may be that only HPH cells with high densities of fusion protein contributed to the measured kinetics. Fusion pores for WT HA cells formed faster at 30°C than at room temperature (our unpublished results), but it was still slower than for HPP* cells at room temperature. In short, whether the presence of a CT affected kinetics depended on the sequence of the TM domain. For P as the TM domain, the P* tail was significantly more effective than the H; for H as a TM domain, the H tail supported fusion, but the P* tail did not.

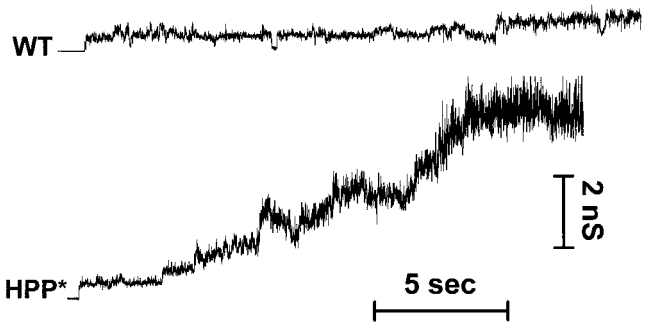


**Figure 8.** Representative patterns of the evolution of conductance of fusion pores formed by WT HA and HPP*. The conductance much more readily increased for HPP*, and pores did not flicker as much as for WT HA. Experiments were performed at room temperature.

### *The Initial Diameter and the Rate of Pore Enlargement Are Affected by the Combination of the TM Domain and CT*

In general, fusion pores induced by HA open instantaneously, exhibiting small conductances, usually $<0.5$ nS, followed by a relatively stable phase, in which the pore conductance did not appreciably increase (Spruce *et al.*, 1991; Zimmerberg *et al.*, 1994). All the chimeras of our study that formed pores (i.e., all but HHP*) did so in this characteristic manner. Pore behavior can be illustrated with representative conductance records of individual experiments (Figure 8). As can be seen, the conductance increased much more readily for HPP* than for WT HA. But conductance trajectories were variable, never identical even for different cells expressing the same construct. We therefore characterized the behavior of a "typical" pore for a given HA construct by averaging the conductance profiles of all fusion pores of that construct (Figure 9, A and B). The initial conductance (Figure 9A) of HPP*-induced (filled triangles) fusion pores ($\sim$0.4 nS) was statistically larger than WT-induced ($\sim$0.2 nS; Figure 9A, open circles) and HEE-induced fusion pores (our unpublished results). Deleting the CT of HPP* (HPstop; Figure 9A, open triangles) resulted in fusion pores with initial conductances indistinguishable from WT HA, whereas HPH (Figure 9A, crossed triangles) created appreciably smaller pores with an initial conductance of $\sim$0.13 nS. Within the first 400 ms after formation (Figure 9A), fusion pores for all constructs did not appreciably enlarge, remaining within the range of their initial conductance. Thus, which combination of CT and TM domain is present clearly affects the initial conductance of fusion pores. For HHP* cells, which exhibited a hemifusion phenotype based on dye spread, fusion pores were not electrically observed for as long as 8–10 min after acidification (our unpublished results).

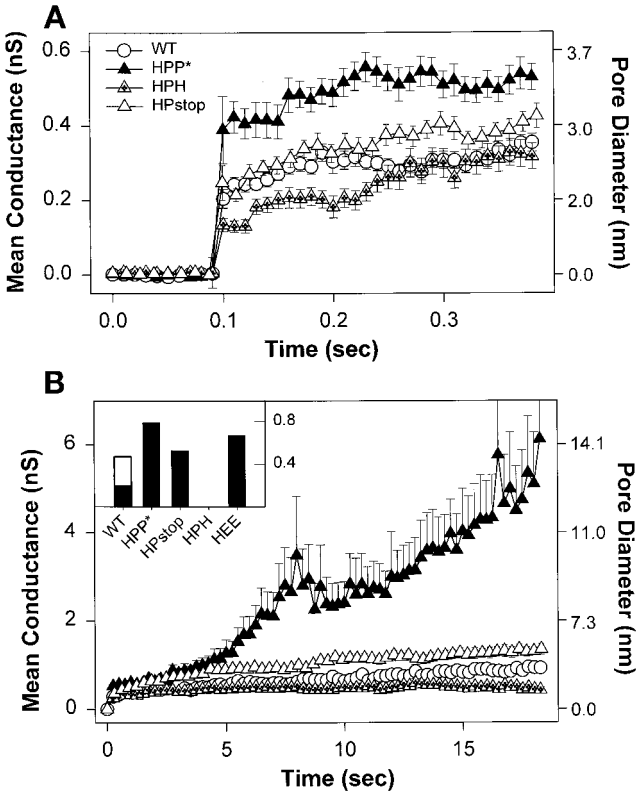


**Figure 9.** Average conductance profiles of pores at early and later times after formation. Pores were aligned at their opening, and the mean and SE of the conductance over time were determined for the entire population of pores. Sample sizes: WT HA (open circles), n = 32; HPP* (filled triangles), n = 20; HPstop (open triangles), n = 28; and HPH (triangles with cross), n = 27. The approximate diameters of fusion pores in nanometers (Spruce *et al.*, 1989) are shown on the right axis. (A) The initial conductance of pores induced by HPP* was statistically ($p < 0.001$) larger than formed by the other constructs. (B) Pores formed by HPP* readily enlarge. Once a pore had increased beyond the measurable range, the conductance for this experiment was artificially fixed at the largest detectable value for purposes of calculating the remainder of the profile. This would cause the calculated average conductance to increasingly underestimate the true value as time advances (see MATERIALS AND METHODS). For visual clarity, one of every 25 points of pore profiles is shown. Inset, The fraction of pores that had enlarged beyond 4 nS in 2 min (error bars are omitted for visual clarity). The enlargement for WT HA-expressing cells at 30°C (open bar, n = 14) was greater than at room temperature (filled bars).

The growth of pores over time also depended on the combination of the TM domain and CT present. WT HA-induced fusion pores often shut and then quickly reopened (Figure 8), a phenomenon known as "flicker" (Spruce *et al.*, 1989; Zimmerberg *et al.*, 1994). WT HA (Figure 9B, open circles) and HPH-induced pores (Figure 9B, triangles with cross) did not grow over 20 s (Figure 9B) and in fact did not enlarge significantly over a 2- to 3-min period (our unpublished results). Pores formed by HPstop (Figure 9B, open triangles) demonstrated a somewhat greater propensity to grow over this 20-s period than WT HA. In contrast, the pore conductance for HPP* cells lingered at small values for only a few seconds (Figures 8 and 9B, filled triangles) before increasing. It reached an average value of >6 nS (~14 nm in diameter) in 20 s and continued to rise. The average fusion pore conductances grew slower for HEE (our unpublished results) than for HPP* but faster than for WT HA. As readily seen by the fraction of fusion pores for each construct that enlarged beyond 4 nS in 2 min (Figure 9B, inset, filled bars), pores formed by HPP* and HPstop more readily enlarged than those formed by WT HA, which in turn more readily enlarged than those formed by HPH.[2] Even at 30°C, WT HA-induced fusion pore conductances (Figure 9B, inset, open bar) increased to a lesser extent than did those created by HPP* at 23°C. This order, overall, parallels the kinetics and efficiency of fusion observed among the constructs.

### *A Point Mutation in the TM Domain of HA Inhibits Fusion*

It had been shown that mutation of either one of the two glycines within the TM domain of the G protein of VSV attenuates the extent of fusion, whereas mutation of both glycines inhibits full fusion but supports hemifusion (Cleverley and Lenard, 1998). The generality of these findings to other fusion proteins was suggested (Cleverley and Lenard, 1998). The HA of the A/Japan/305/57 strain used in the present study has two glycines within its TM domain; the one at position 530 is conserved among strains of influenza, whereas the glycine at position 520 (Figure 1) is a serine in most other strains. We made three separate point mutations. Two were at G520, either to serine (G520S) or to leucine (G520L), and the third was at G530 to tryptophan (G530W).

Mutating the conserved G530 did not affect fusion: both lipid and aqueous dyes efficiently redistributed from RBCs (Figure 10, A and B). Because position 520 is usually a serine and conserved among most strains of influenza, it is significant that the mutation G520S had no affect on the efficacy of fusion (Figure 10, C and D). In contrast, fusion activity for G520L was dramatically attenuated: R18 redistributed into only a few HA cells (Figure 10E), and aqueous dye transfer was virtually absent (Figure 10F). G520L was properly folded (Figure 2B, lane 4) and was expressed on cell

[2] The electrically measured pore conductance is the total conductance of all pathways connecting two fused cells. Thus, increases in pore conductance need not occur only by pore enlargement. Successive formation of multiple pores will also result in conductance increases (Zimmerberg *et al.*, 1994). However, pore growth measured by either differential sieving of fluorescent dyes or by increases in total conductance were in accord in our study. This supports our conclusion that pores formed by the different constructs actually grow at different rates.

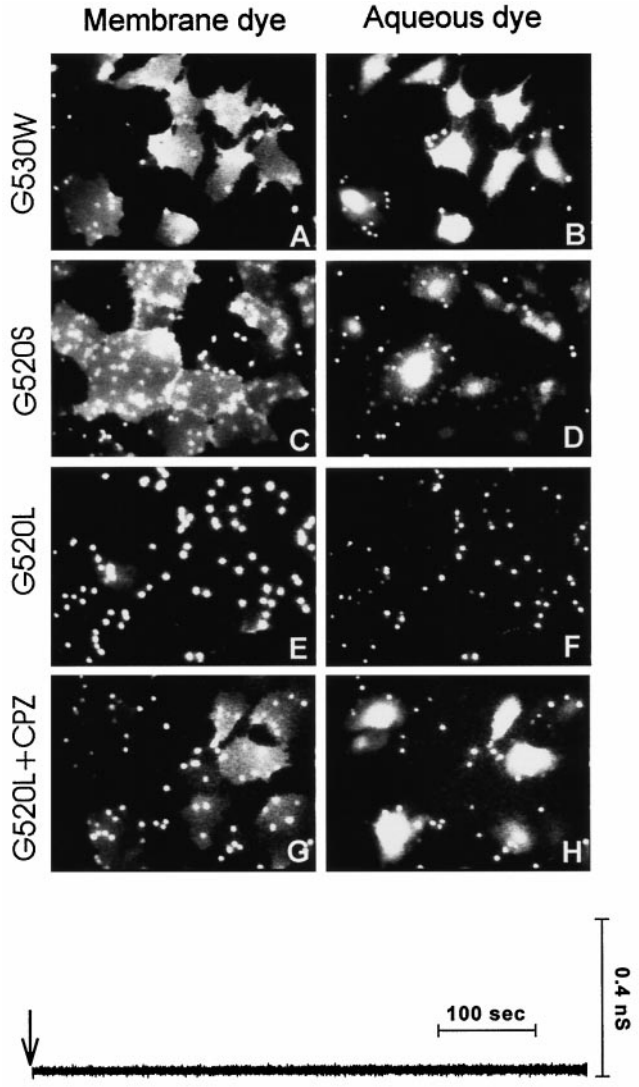


**Figure 10.** Fusion activity of the point mutants G520L HA, G520S HA, and G530W HA. Fusion of bound RBCs colabeled with CF and R18 to HA cells was triggered by application of a pH 4.8 solution at 37°C for 2 min and then incubating the cells for 10 min at room temperature in PBS supplemented with raffinose. The G530W mutant induced efficient redistribution of both dyes (A and B). G520S HA was also effective in promoting fusion (C and D). Very little lipid dye mixing (E) and virtually no aqueous dye redistribution (F) was observed for the G520L mutant. Subsequent application of 0.5 mM CPZ to the G520L-expressing cells resulted in extensive transfer of both CF (H) and R18 (G). The electrical trace ($Y_0$) illustrates that pores did not form for G520L after the low-pH pulse (downward arrow). However, a rare transient opening of a fusion pore followed by its closing was sometimes detected when the probability of pore formation was increased by binding many RBCs to the G520L cells.

surfaces at the same density as WT HA (Table 1) and bound RBCs as effectively. For the few G520L HA cells into which R18 did redistribute, the labeling was faint, indicating that dye movement was restricted. The absence of fusion pores was rigorously demonstrated by electrical capacitance measurements: pores had not formed with the G520L mutant by 10 min after exposure to pH 4.8 at room temperature (Figure 10, electrical trace).

When membranes have hemifused (as evidenced by spread of lipid dye), CPZ promotes fusion (Melikyan *et al.*, 1997a). CPZ promotes fusion when membranes have reached a state intermediate to fusion (thought to be local hemifusion), even before mixing of lipid dye (Chernomordik *et al.*, 1998). After acidification and reneutralization of G520L cells bound to RBCs, a brief application of CPZ quickly caused efficient transfer of both R18 and CF into the majority of the cells (Figure 10, G and H). This shows that the G520L mutant had undergone a low-pH–induced conformational change that allowed the membranes to approach each other and suggests that they may have locally hemifused without permitting passage of lipid dye, referred to as "restricted hemifusion" (Chernomordik *et al.*, 1998). Thus, although a TM domain from proteins unrelated to fusion can support fusion, a point mutation at a critical location within the TM domain of HA can arrest the process.

## DISCUSSION

### *Fusion Occurs When the Ectodomain of HA Is Anchored to Membranes with a Foreign TM Domain but Is Modulated by the Sequence of the CT*

We have shown that the TM domain of a nonviral, nonfusion integral membrane protein, pIgR, can substitute for that of HA and still cause fusion. Similar findings have been obtained using chimeras between the ectodomains of either G protein of VSV (Odell *et al.*, 1998) or gp160 (the fusion protein) of human immunodeficiency virus (Wilk *et al.*, 1996) and the TM domain and CT from proteins unrelated to fusion. Furthermore, TM domains and CTs derived from other viral fusion proteins can effectively substitute for those of HA (Roth *et al.*, 1986; Dong *et al.*, 1992; Schroth-Diez *et al.* 1998). We therefore conclude that it is generally the case that the TM domain does not need to fulfill stringent sequence requirements for fusion to occur.

Nevertheless, we found that the point mutation G520L within the TM domain of HA significantly inhibits full fusion. Also, point mutations within the TM domain of the G protein of VSV inhibit fusion, indicating that certain residues within a TM domain can play a critical role in whether fusion proceeds (Cleverly and Lenard, 1998). At first glance it would seem odd or even contradictory that a specific residue within the TM domain is important for fusion, whereas the overall amino acid sequence of the domain is not. It is noteworthy too that the efficacy of fusion for HA chimeras depended not only on the TM

domain but on that TM domain's association with a particular CT. In other words, although a CT is not required for HA-mediated fusion, when present, its alteration can affect fusion to the point of abolishing it (Figure 5; Ohuchi *et al.*, 1998). What could account for these findings?

A point mutation or chimera can create different propensities for or against residing in rafts of cholesterol complexed with sphingomyelin (Schieffele *et al.*, 1997); if rafts have an effect on the fusion process, this propensity could be an important factor. It is unlikely, however, that rafts do have an effect on the fusion process. There was no correlation between affinity for a raft and ability to promote fusion. Neither HPP* (optimal for fusion) nor HPH (less effective than WT HA) resided within rafts (Figure 2C). Both were effectively solubilized by Triton X-100 at 4°C. Also, depleting WT HA cells of cholesterol eliminated rafts without affecting pore formation or growth (Figure 5). Therefore, not only can the amino acid sequence of the TM domain significantly vary without hindering the fusion process, but the lipid environment of the TM domain can vary without hindrance as well.

Alternatively, the ability to undergo low-pH–induced conformational changes could depend on the combination of the TM domain and CT. This also appears unlikely. The chimeras and mutants were folded and expressed properly (Figure 2 and Table 1). The pH dependence of fusion shifted only 0.2 units toward more acidic values than WT HA (Figure 4). This may indicate that either the chimeras were stabilized somewhat against low-pH conformational changes (Steinhauer *et al.*, 1991) or more trimers were required to form a pore than for WT HA.

Considering the unlikelihood of the above possibilities, we propose that the explanation is a basic structural one, because function (in this case, fusion) follows from structure. There is probably some structure that the TM domain must be able to assume, during at least some stage in the process, to cause fusion. The ability to assume this structure can be affected by mutation within the TM domain itself or by the sequence within the CT. The required structural motif would have to be rather common among TM domains, because a foreign TM domain can support fusion. The finding that G520S HA causes fusion, but G520L does not, provides a natural explanation for the fact that residue 520 is rather well conserved, usually a serine (although a glycine in Japan 57 HA).

The TM domain and CT of fusion proteins may not be independent structural entities. Chimeras for which the TM domain and CT were derived from the same protein, either HA or pIgR, were more effective in promoting fusion by every criteria—efficiency and kinetics of pore formation and pore enlargement—than were the chimeras with the two domains derived from different proteins. At the extremes, HPP* was optimal, but HHP* did not support fusion. The HEE chimera was also effective in promoting pores that readily enlarged. Thus the amino acid sequences of the TM domain and CT may have to be compatible with each other to preserve an overall structure, and the observed functional coupling between these domains may be a reflection of this structural necessity.

### *Biological Ramifications of the Role of the CT on the Fusion Protein*

The finding that HPP* and HPstop have greater ability to cause fusion than WT HA shows that the TM domain and CT of HA have not evolved to simply optimize fusion. This makes sense because HA must fulfill functions other than fusion as part of the viral life cycle, including proper sorting within a host cell (Lin *et al.*, 1998) and assembly and budding of viral particles (Jin *et al.*, 1994). Furthermore, although the presence of a CT does not strongly affect fusion, it may be required for other influenza viral functions, because virus has been shown to try to maintain its CT; influenza virus engineered (by inserting a single stop codon) to have a tailless HA eventually reverts to virus whose HA contains a restored CT (Jin *et al.*, 1994).

Although the CT is not required for HA-mediated fusion in influenza, for some other viruses its presence is known to be essential (Bagai *et al.*, 1996). For many viruses, including influenza (Ohuchi *et al.*, 1998), altering the fusion protein's CT can strongly affect fusion (Chakrabarti *et al.*, 1989; Mulligan *et al.*, 1992; Johnson *et al.*, 1993; Ritter *et al.*, 1993; Owens *et al.*, 1994; Spies and Compans, 1994; Sergel and Morrison, 1995). In the case of the retrovirus Moloney murine leukemia virus, the fusion protein is synthesized with a long CT and cannot cause fusion. The virus itself, through its own protease, shortens the CT to activate the protein only after viral assembly has taken place at the plasma membrane of the infected cell (Rein *et al.*, 1994; Januszeski *et al.*, 1997). That is, as part of its natural life cycle, this retrovirus controls the identity of its CT, thereby ensuring that fusion can occur only when the virus is assembled, ready to infect other cells. It may be that for viral fusion proteins in general, the CT does not directly contribute to fusion. But its length and sequence must be compatible with the TM domain and/or ectodomain to allow them to assume conformations required for fusion.

### *The Wide Latitude in Functional Amino Acid Sequences in the TM Domain Supports the Hemifusion Model*

There is a possible mechanism of fusion in which hemifusion is not an intermediate stage: the initial pore is formed by and solely composed of fusion proteins that connect the two membranes (Tse *et al.*,

1993; Lindau and Almers, 1995). In this scenario, aqueous continuity is established before any lipid monolayer merger. There is a precedent for this structure: a gap junction composed solely of protein connecting two membranes. The findings that GPI-HA causes hemifusion are consistent with both hypotheses. In a hemifusion mechanism, the TM domain would be required to disrupt the hemifusion diaphragm to create a pore that would connect aqueous compartments. If, on the other hand, the pore were composed solely of protein, the TM domain of HA would be needed to form the wall of the pore within the HA-expressing membrane. But proteins that form water-filled pores have fairly strict amino acid sequence requirements over the extensive lumenal region because of polarity considerations. The sequence requirements of this model are inconsistent with our findings; in fact it would be unprecedented if a TM domain composed of virtually any amino acid sequence could line the lumen of a water-filled pore.

The finding that a wide range of TM sequences are effective in fusion strongly supports the hypothesis that the fusion proteins first induce hemifusion by acting on contacting (outer) monolayers. Hemifusion must be initiated at a local site (Figure 11, local or restricted hemifusion), probably through the formation of a stalk (Chernomordik *et al.*, 1995). The TM domains of the fusion proteins that buttress this structure could then physically destabilize the hemifusion diaphragm by a mechanism with little sequence requirement. The TM domain could insert into the diaphragm, inducing the lipids that constitute the diaphragm to reestablish the transmembrane orientation of this domain by reconfiguring around it into a pore. Or the TM domains may pull out on the diaphragm and thereby generate a membrane tension that ruptures the diaphragm. In either case, a small pore that can still close forms within the local hemifusion diaphragm (Figure 11, reversible opening of a fusion pore). Once the pore opens sufficiently, it remains open and eventually fully enlarges.

The observed variation of kinetics of fusion with differing TM domains and CTs (Figure 7) suggests that destabilization of the local hemifusion diaphragm may be a rate-limiting step. In general, if transition from one state to another is rate limiting, the original state will be relatively stable. Thus local hemifusion may constitute a configuration separated from the fusion pore by an energetic barrier. If this is the case, it should be possible to arrest the fusion process at that state. After exposing G520L cells bound to RBCs to low pH, lipid dye did not spread, but subsequent addition of CPZ at neutral pH caused both lipid and aqueous dye transfer (Figure 10). Because this is the "fingerprint" expected of restricted hemifusion (Chernomordik *et al.*, 1998), we conclude that G520L is not completely nonfunctional but has locked the mem-

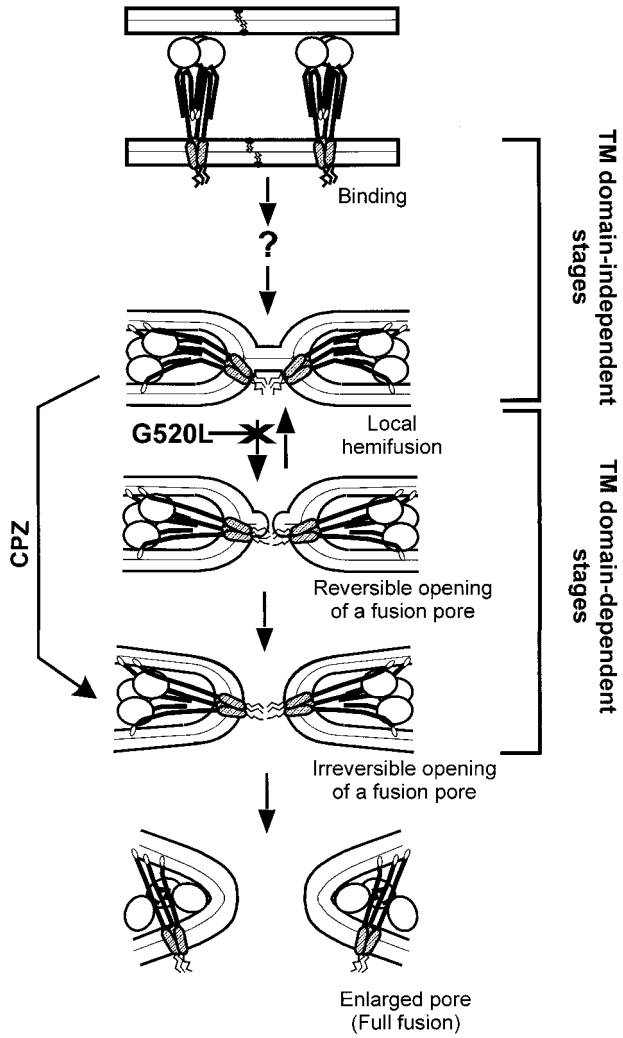


**Figure 11.** Schematic representation of the progression through intermediates in HA-mediated fusion. Each monomer of the HA homotrimer consists of HA1 (shown as a globular head with a short "tail") and HA2 (a membrane-anchored polypeptide) subunits. The fusion peptides (small open ellipses) are initially sequestered from aqueous phase. Each TM domain is represented by a larger ellipse, and a CT is shown by thin lines. The HA-expressing cell binds to its target membrane (Binding) via specific interactions between the HA1 subunit and sialates on the target membrane. Low pH triggers a series of conformational changes in HA that result in insertion of fusion peptides into viral and target membranes. Fusion probably proceeds from a local membrane merger (Local hemifusion) mediated by the ectodomain of HA. The question mark between the bound and hemifused states denotes that the manner by which HA causes this initial hemifusion is not known. The addition of CPZ converts the local hemifusion intermediate to a pore that has irreversibly opened (Irreversible opening of a fusion pore), effectively bypassing the small flickering pore (Reversible opening of a fusion pore). We propose that for membranes in the state of local hemifusion the combination of the TM domain and CT causes the destabilization of the hemifusion diaphragm that results in an initial pore that can still close. After some enlargement the pore remains open and eventually fully enlarges (Enlarged pore). Stages up to local hemifusion do not require the presence of a TM domain, whereas pore formation does.

branes in a state of local hemifusion.[3] In our model the ectodomain causes hemifusion independent of the TM domain; the TM domain is responsible for destabilizing the hemifusion diaphragm (Figure 11). It is thus notable that a point mutation within the TM domain arrests fusion at the stage of local hemifusion.

Even when a small pore has formed between an HA cell and an RBC (and therefore all monolayers should have merged), lipid does not appear to move from one membrane to the other (Tse *et al.*, 1993; Zimmerberg *et al.*, 1994). Therefore, lipid dye is not expected to move (hence the term restricted) in the earlier stage of local hemifusion (Chernomordik *et al.*, 1998). Within the context of the model (Figure 11), protein forms a ring at the point of hemifusion (Monck and Fernandez, 1992; Chernomordik *et al.*, 1998), and even after the formation of a small pore, this ring blocks lipid movement. Lipids insinuate themselves into the ring as HA trimers move apart; this is observed as both pore enlargement and lipid dye movement (Tse *et al.*, 1993; Hernandez *et al.*, 1996; Chernomordik *et al.*, 1998). The different initial pore conductances between chimeras (Figure 9) would be expected if the average protein stoichiometry within the ring depended on the combination of TM domain and CT. That is, the capacity of chimeric HA trimers to associate with each other may depend on the amino acid sequence of the TM domain. Because pore growth should depend on the ability of fusion proteins to separate from each other, enlargement would be expected to vary with the TM domain and CT; this is experimentally observed (Figures 5 and 9).

We are thus led to the view that for WT HA the ectodomain alone is responsible for hemifusion, without participation of the TM domain. The function of the TM domain is in some way to destabilize the hemifusion diaphragm, leading to pore formation; this step depends on and is subsequent to hemifusion.

## ACKNOWLEDGMENTS

We thank Sofya Brener and Katrina Latham for sustained and excellent technical assistance, Dr. Thomas Braciale for supplying FC-125 mAb, Dr. Gregory Spear and Jocelyn Jacubik for use of their flow cytometer, and Drs. Vladimir Ratinov and Joshua Zimmerberg for the lock-in amplifier software. This work was supported by National Institutes of Health grants GM-27367, GM-37547, and GM-54787.

## REFERENCES

Bagai, S., and Lamb, R.A. (1996). Truncation of the COOH-terminal region of the paramixovirus SV5 fusion protein leads to hemifusion but not complete fusion. J. Cell Biol. *135*, 73–84.

[3] The TM domain of pIgR also contains, by coincidence, a glycine at position 520 (Figure 1). This residue should clearly be mutated as part of a future study to further determine the details of the TM domain sequence requirements necessary for fusion.

Blumenthal, R., Sarkar, D.P., Durell, S., Howard, D.E., and Morris, S.J. (1996). Dilation of the influenza hemagglutinin fusion pore revealed by the kinetics of individual cell-cell fusion events. J. Cell Biol. *135*, 63–71.

Brown, D.A., and London, E. (1997). Structure of detergent-resistant membrane domains: does phase separation occur in biological membranes? Biochem. Biophys. Res. Commun. *240*, 1–7.

Bullough, P.A., Hughson, F.M., Skehel, J.J., and Wiley, D.C. (1994). Structure of influenza hemagglutinin at the pH of membrane fusion. Nature *371*, 37–43.

Chakrabarti, L., Emerman, M., Tiollais, P., and Sonigo, P. (1989). The cytoplasmic domain of simian immunodeficiency virus transmembrane protein modulates infectivity. J. Virol. *63*, 4395–4403.

Chan, D.C., Fass, D., Berger, J.M., and Kim, P.S. (1997). Core structure of gp41 from the HIV envelope glycoprotein. Cell *89*, 263–273.

Chernomordik L.V., Frolov, V.A., Leikina, E., Bronk, P., and Zimmerberg, J. (1998). The pathway of membrane fusion catalyzed by influenza hemagglutinin: restriction of lipids, hemifusion, and lipidic fusion pore formation. J. Cell Biol. *140*, 1369–1382.

Chernomordik, L.V., Kozlov, M.M., and Zimmerberg, J. (1995). Lipids in biological membrane fusion. J. Membr. Biol. *146*, 1–14.

Cleverley, D.Z., and Lenard, J. (1998). The transmembrane domain in viral fusion: essential role for a conserved glycine residue in vesicular stomatitis virus G protein. Proc. Natl. Acad. Sci. USA *95*, 3425–3430.

Copeland, C.S., Doms, R.W., Bolzau, E.M., Webster, R.G., and Helenius, A. (1986). Assembly of influenza hemagglutinin trimers and its role in intracellular transport. J. Cell Biol. *103*, 1179–1191.

Dong, J., Roth, M.G., and Hunter, E. (1992). A chimeric avian retrovirus containing the influenza virus gene has an expanded host range. J. Virol. *66*, 7374–7382.

Durell, S.R., Martin, I., Ruysschaert, J.M., Shai, Y., and Blumenthal, R. (1997). What studies of fusion peptides tell us about viral envelope glycoprotein-mediated membrane fusion. Mol. Membr. Biol. *14*, 97–112.

Ellens, H., Doxsey, S., Glenn, J.S., and White, J.M. (1989). Delivery of macromolecules into cells expressing a viral membrane fusion protein. Methods Cell Biol. *31*, 155–176.

Friedrichson, T., and Kurzchalia, T.V. (1998). Microdomains of GPI-anchored proteins in living cells revealed by cross-linking. Nature *394*, 802–805.

Gething M.-J., McCammon, K., and Sambrook, J. (1986). Expression of wild-type and mutant forms of influenza hemagglutinin: the role of folding in intracellular transport. Cell *46*, 939–950.

Gillis, K.D. (1995). Techniques for membrane capacitance measurements. In: Single-Channel Recording, ed. B. Sakmann and E. Neher, New York: Plenum Press, 155–198.

Hernandez, L.D., Hoffman, L.R., Wolfberg, T.G., and White, J.M. (1996). Virus-cell and cell-cell fusion. Annu. Rev. Cell Dev. Biol. *12*, 627–661.

Januszeski, M.M., Cannon, P.M., Chen, D., Rozenberg, Y., and Anderson, W.F. (1997). Functional analysis of the cytoplasmic tail of Moloney murine leukemia virus envelope protein. J. Virol. *71*, 3631–3619.

Jin, H., Leser, G.P., and Lamb, R.A. (1994). The influenza virus hemagglutinin cytoplasmic tail is not essential for virus assembly or infectivity. EMBO J. *13*, 5504–5515.

Johnston, P.B., Dubay, J.W., and Hunter, E. (1993). Truncations of the simian immunodeficiency virus transmembrane protein confer

expanded virus host range by removing a block to virus entry into cells. J. Virol. *67*, 3077–3086.

Joshi, C., and Fernandez, J.M. (1988). Capacitance measurements. An analysis of the phase detector technique used to study exocytosis and endocytosis. Biophys. J. *53*, 885–892.

Kemble, G.W., Danieli, T., and White, J.M. (1994). Lipid-anchored influenza hemagglutinin promotes hemifusion, not complete fusion. Cell *76*, 383–391.

Kemble, G.W., Henis, Y.I., and White, J.M. (1993). GPI- and transmembrane-anchored influenza hemagglutinin differ in structure and receptor binding activity. J. Cell Biol. *122*, 1253–1265.

Lazarovits, J., Shia, S.P., Ktistakis, N., Lee, M.S., Bird, C., and Roth, M.G. (1990). The effects of foreign transmembrane domains on the biosynthesis of the influenza virus hemagglutinin. J. Biol. Chem. *265*, 4760–4767.

Lin, S., Naim, H.Y., Rodriguez, A.C., and Roth, M.G. (1998). Mutations in the middle of the transmembrane domain reverse the polarity of transport of the influenza virus hemagglutinin in MDCK epithelial cells. J. Cell Biol. *142*, 51–57.

Lindau, M. (1991). Time-resolved capacitance measurements: monitoring exocytosis in single cells. Q. Rev. Biophys. *24*, 75–101.

Lindau, M., and Almers, W. (1995). Structure and function of fusion pore in exocytosis and ectoplasmic membrane fusion. Curr. Opin. Cell Biol. *7*, 509–517.

Melikyan, G.B., Brener, S.A., Ok, D.C., and Cohen, F.S. (1997a). Inner but not outer membrane leaflets control the transition from glycosylphosphatidylinositol-anchored influenza hemagglutinin-induced hemifusion to full fusion. J. Cell Biol. *136*, 995–1005.

Melikyan, G.B., Jin, H., Lamb, R.A., and Cohen, F.S. (1997b). The role of the cytoplasmic tail region of influenza virus hemagglutinin in formation and growth of fusion pores. Virology *235*, 118–128.

Melikyan, G.B., White, J.M., and Cohen, F.S. (1995). GPI-anchored influenza hemagglutinin induces hemifusion to both red blood cell and planar bilayer membranes. J. Cell Biol. *131*, 679–691.

Monck, J.R., and Fernandez, J.M. (1992). The exocytotic fusion pore. J. Cell Biol. *119*, 1395–1404.

Mostov K.E., Friedlander, M., and Blobel, G. (1984). The receptor for transepithelial transport of IgA and IgM contains multiple immunoglobulin-like domains. Nature *308*, 37–43.

Mulligan M.J., Yamshchikov, G.V., Ritter, G.D., Jr., Gao, F., Jin, M.J., Nail, C.D., Spies, C.P., Hahn, B.H., and Compans, R.W. (1992). Cytoplasmic domain truncation enhances fusion activity by the exterior glycoprotein complex of human immunodeficiency virus type 2 in selected cell types. J. Virol. *66*, 3971–3975.

Naim, H.Y., and Roth, M.G. (1993). Basis for selective incorporation of glycoproteins into the influenza virus envelope. J. Virol. *67*, 4831–4841.

Naim, H.Y., and Roth, M.G. (1994). SV40 virus expression vectors. Methods Cell Biol. *43*, 113–136.

Neher, E., and Marty, A. (1982). Discrete changes of cell membrane capacitance observed under conditions of enhanced secretion in bovine adrenal chromaffin cells. Proc. Natl. Acad. Sci. USA *79*, 6712–6716.

Nüssler, F., Clague, M.J., and Herrmann, A. (1997). Meta-stability of the hemifusion intermediate induced by glycosylphosphatidylinositol-anchored influenza hemagglutinin. Biophys. J. *73*, 2280–2291.

Odell, D., Wanas, E., Yan, J., and Ghosh, H. (1997). Influence of membrane anchoring and cytoplasmic domains on the fusogenic activity of vesicular stomatitis virus glycoprotein G. J. Virol. *71*, 7996–8000.

Ohuchi, M., Fischer, C., Ohuchi, R., Herwig, A., and Klenk, H.D. (1998). Elongation of the cytoplasmic tail interferes with the fusion activity of influenza virus hemagglutinin. J. Virol. *72*, 3554–3559.

Owens, R.J., Burke, C., and Rose, J.K. (1994). Mutations in the membrane-spanning domain of the human immunodeficiency virus envelope glycoprotein that affect fusion activity. J. Virol. *68*, 570–574.

Poirie, M.A., Xiao, W., Macosko, J.C., Chan, C., Shin, Y.K., and Bennett, M.K. (1998). The synaptic SNARE complex is a parallel four-stranded helical bundle. Nat. Struct. Biol. *5*, 765–769.

Ratinov V., Plonsky, I., and Zimmerberg, J. (1998). Fusion pore conductance: experimental approaches and theoretical algorithms. Biophys. J. *74*, 2374–2387.

Rein, A., Mirro, J., Haynes, J.G., Ernst, S.M., and Nagashima, K. (1994). Function of the cytoplasmic domain of a retroviral transmembrane protein: p15E-p2E cleavage activates the membrane fusion capability of the murine leukemia virus env protein. J. Virol. *68*, 1771–1781.

Ritter, G.D., Mulligan, M.J., Lydy, S.L., and Compans, R.W. (1993). Cell fusion activity of the simian immunodeficiency virus envelope protein is modulated by the intracytoplasmic domain. Virology *197*, 255–264.

Roth, M.G., Doyle, C., Sambrook, J., and Gething, M.-J. (1986). Heterologous transmembrane and cytoplasmic domains direct functional chimeric influenza virus hemagglutinins into the endocytic pathway. J. Cell Biol. *102*, 1271–1283.

Sarkar, G., and Sommer, S.S. (1990). The "Megaprimer" method of site-directed mutagenesis. Biotechniques *8*, 404–407.

Schieffele, P., Roth, M.G., and Simons, K. (1997). Interaction of influenza virus hemagglutinin with sphingolipid-cholesterol membrane domains via its transmembrane domain. EMBO J. *16*, 5501–5508.

Schroth-Diez, B., Ponimaskin, E., Reverey, H., Schmidt, M.F., and Herrmann, A. (1998). Fusion activity of transmembrane and cytoplasmic domain chimeras of the influenza virus glycoprotein hemagglutinin. J. Virol. *72*, 133–141.

Sergel, T., and Morrison, T.G. (1995). Mutations in the cytoplasmic domain of the fusion glycoprotein of Newcastle disease virus depress syncytia formation. Virology *210*, 264–272.

Simons, K., and Ikonen, E. (1997). Functional rafts in cell membranes. Nature *387*, 569–572.

Spies, P.C., and Compans, R.W. (1994). Effect of cytoplasmic domain length on cell surface expression and syncytium-forming capacity of the simian immunodeficiency virus envelope glycoprotein. Virology *203*, 8–19.

Spruce, A.E., Iwata, A., and Almers, W. (1991). The first milliseconds of the pore formed by a fusogenic viral envelope protein during membrane fusion. Proc. Natl. Acad. Sci. USA *88*, 3623–3627.

Spruce, A.E., Iwata, A., White, J.M., and Almers, W. (1989). Patch clamp studies of single cell-fusion events mediated by a viral fusion protein. Nature *342*, 555–558.

Steinhauer, D.A., Wharton, S.A., Skehel, J.J., Wiley, D.C., and Hay, A.J. (1991). Amantadine selection of a mutant influenza virus containing an acid-stable hemagglutinin glycoprotein: evidence for virus-specific regulation of the pH of glycoprotein transport vesicles. Proc. Natl. Acad. Sci. USA *88*, 11525–11529.

Stegmann,T., White, J.M., and Helenius, A. (1990). Intermediates in influenza induced membrane fusion. EMBO J. *9*, 4231–4241.

Südhof, T.C. (1995). The synaptic vesicle cycle: a cascade of protein-protein interactions. Nature *375*, 645–653.

Sutton, R.B., Fasshauer, D., Jahn, R., and Brunger, A.T. (1998). Crystal structure of a SNARE complex involved in synaptic exocytosis at 2.4 A resolution. Nature *395*, 347–353.

Tse, F.W., Iwata, A., and Almers, W. (1993). Membrane flux through the pore formed by a fusogenic viral envelope protein during cell fusion. J. Cell Biol. *121*, 543–552.

Varma, R., and Mayor, S. (1998). GPI-anchored proteins are organized in submicron domains at the cell surface. Nature *394*, 798–801.

Wang, H.-Z., and Veenstra, R.D. (1997). Monovalent ion selectivity sequences of the rat connexin43-gap junction. J. Gen. Physiol *109*, 491–507.

Wilk, T., Pfeiffer, T., Bukovsky, A., Moldenhauer, G., and Bosch, V. (1996). Glycoprotein incorporation and HIV-1 infectivity despite exchange of the gp160 membrane-spanning domain. Virology *218*, 269–274.

Wilson, I.A., Skehel, J.J., and Wiley, D.C. (1981). Structure of the hemagglutinin membrane glycoprotein of influenza virus at 3 Å resolution. Nature *289*, 366–373.

Zimmerberg, J., Blumenthal, R., Sarkar, D.P., Curran, M., and Morris, S.J. (1994). Restricted movement of lipid and aqueous dyes through pores formed by influenza hemagglutinin during cell fusion. J. Cell Biol. *127*, 1885–1894.